Contemporary Engineering Sciences, Vol. 2, 2009, no. 2, 47 - 58

Attenuation and Time Dispersion Measurements of Graded Index Polymer Optical Fiber for Indoor Cellular Coverage

S. Louvros and I. E. Kougias

Department of Telecommunication Systems and Networks (TESYD)
Technological Educational Institute of Messolonghi, Greece
splouvros@gmail.com, kougias@teimes.gr

Abstract

Grated Index Polymer Optical Fiber (GI-POF) is of great interest the last decade, mainly for short distance applications. UMTS in-building cellular coverage could use POF transmission networks taking advantage of its cost effective deployment and its high data rate for in-building distances. Based on a generalized impulse response of multimode channel, a method for GI-POF channel characterization (time response evaluation) is used and evaluations based on analytical model calculations and computer simulations are performed.

Keywords: Grated Index Polymer Optical Fiber, transmission networks

1. Introduction

In nowadays cellular networks with heterogeneous general network structure in different traffic capacity regions (city centres, train/subway platforms, indoor/in-building dedicated capacity), an overall system network design should be considered. Especially in the radio access network a multilayer coverage has been provided in order to incorporate all the different scenario of capacity demand, with one special scenario the indoor pico-cellular coverage which can emerge for several reasons, mainly the capacity and quality. For example if the in-building coverage is poor from outside cells, leading to bad quality, a solution could be an indoor dedicated cellular network, as shown in figure 1.

Fig. 1 Indoor cellular coverage

Buildings generating a high traffic load, such as conference centres and airports, may need in-building systems to take care of the traffic. A different application is the business in-building system with the aim to complement or replace the fixed telephony network. The aim of in-building cell planning is, to plan for good coverage and capacity, and at the same time interfere as little as possible. Special antenna technology is designed and the power level is minimized so much as to satisfy the indoor propagation models. Moreover, it is important to also consider a preparation for any future extension of the indoor transmission system, both from a coverage point of view (more available frequencies and antenna pending positions for future expansion), as well as from a capacity point of view (available pending infrastructure such as fiber terminations, optical connectors and transmission capacity in the building to be provided in advance [1]). Inside a building the antenna transmission and distribution network is very important since the cost of the installation can be optimized regarding the application, figure 2. The antenna distribution and transmission configurations for in-building applications can be divided into distributed antennas using a coax feeder network, radiating cable, and distributed antennas using a fiber-optical network. There are different solutions based on fiber-optics that can be used for in-building systems. The main purpose though is to overcome losses in long coaxial feeder cables. The major disadvantage of using a fiber-optical network is that each antenna terminal requires local power supply and alarm handling. Note that an additional fiber-optical antenna requires the installation of two additional transmitter/receiver fibers all the way from the optical interface unit to the location of the antenna, due to the RF-to-optical conversion. Ordinary antennas may, however, be connected to the external antenna terminal on the fiber-optical antenna. Generally in the international literature there are several applications based on Silica - single mode optical fiber for long distances supporting Gbps transmission rates due to its high bandwidth.

Multimode optical fibers are also of great interest in local area networks (LANs) and interconnections with moderate transmission rates due to its large core diameter facilitating the connection expenses. However, one of the latest technology advances called Polymer Optical Fiber (POF), with relative larger core diameters (100–1000 microns) enables the use of inexpensive polymer connectors without any serious influence on the coupling loss [2-3] and reducing the modal noise in the multimode transmission for shorter distances. This is due to the high attenuation behaviour of the PolyMethyl-MethAcrylate (PMMA) POF fibers [5] (100 dB/Km in the visible wavelengths) compared to Silica fibers, a characteristic that could be a disadvantage but in our case for indoor applications could be an advantage from the flexibility and cost efficiency deployment point of view [6]. Moreover, in order to improve the transmission characteristics of PMMA POF, Graded Index profiles (GI-PMMA POF) is proposed [7].

In the international literature, existing POF channel modeling deal so far with the calculation of the input pulse broadening from the moments of the impulse response [8-10], or the direct evaluation of the frequency response [11-12]. In [12] a different method, based on the definition of impulse response for multimode channels, was proposed and used to calculate analytically the time response. It is a method for end-to-end system modeling and evaluation of POF, also including the light source as a different channel model. Both chromatic (intramodal) and intermodal dispersions were taken into account and Differential Mode Attenuation (DMA) was included [10] in the evaluation while mode coupling was not considered as it has been proven to be negligible for GIPOF [11,12].

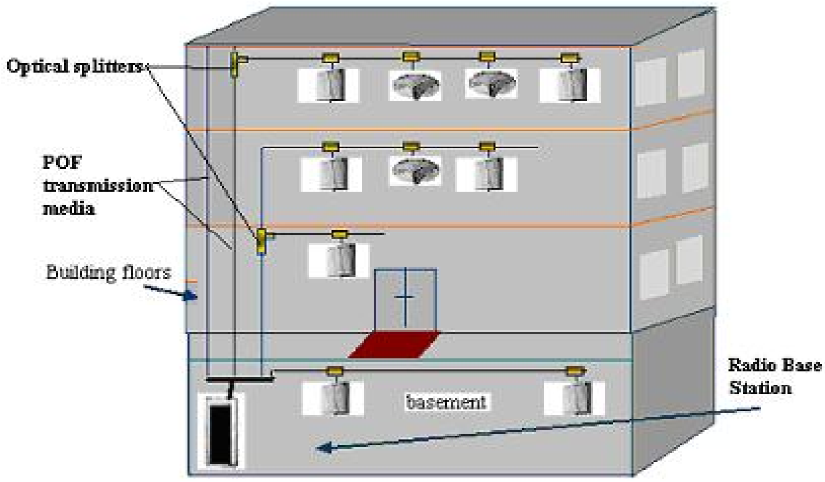

Fig. 2 The indoor transmission system

2. The Analytical Model

After certain mathematical analysis [8] and also considering the band-pass optical output spectral width $[\lambda_1, \lambda_2]$ characteristics of a light LED source, the band-pass impulse response was calculated as:

$$h(t,z) = \sum_{m=1}^{M(t)} A_m[T_m^{(-1)}(t), z] \cdot \frac{dT_m^{(-1)}(t)}{dt}, \quad \lambda_1 \leq \lambda \leq \lambda_2, \tag{1}$$

where $A_m(\lambda, z)$ [8] is the mode's power in mode group *m,* wavelength λ and distance *z.* Equation (1) gives the response in terms of time delay and distance and $M(t)$ is the number of mode groups contributing to the response at instant *t* for each wavelength λ [8]. $T_m(\lambda)$ is the modal delay per unit length [11,12]:

$$T_m(\lambda) = \frac{N_1(\lambda)}{c}\left[1 - \frac{\Delta(\lambda)[1+\varepsilon(\lambda)]}{\alpha+2}\left(\frac{m}{M(\lambda)}\right)^{\frac{2\alpha}{\alpha+2}}\right] \cdot \left[1 - 2\Delta(\lambda)\left(\frac{m}{M(\lambda)}\right)^{\frac{2\alpha}{\alpha+2}}\right]^{-\frac{1}{2}}. \tag{2}$$

For each mode group response, the response of the individual modes is summed, their number being calculated as the sum of all modes satisfying $m = 2m + n$, where m and n denote the radial and azimuthal nodes, respectively, of the mode [10]. For the evaluation region under consideration, the inverse modal delay function $T_m^{-1}(t)$ in (1), for each mode group, must be calculated, where the number of excited mode groups per wavelength is [11,12]:

$$M(\lambda) = 2\pi w \frac{n_1(\lambda)}{\lambda}\left(\frac{\alpha\Delta(\lambda)}{\alpha+2}\right)^{1/2} \tag{3}$$

and the time window of each mode group corresponding to wavelengths λ_1 and λ_2 is calculated. Then an inverse function per mode can be numerically calculated from (5) for the time samples under consideration. For a given time instant *t* in the time response window, and for a specific mode group, the wavelength that results in a response at this instant is calculated using the inverse modal delay function. If this wavelength is in the evaluation region the attenuation of the mode is encountered in the response. In case the wavelength is out of the evaluation region, the response is not taken into account. This procedure is repeated for the maximum number of excited mode groups $M(\lambda)$ in the evaluation wavelength region. Modal attenuation can be described by:

$$A_m(\lambda, z) = e^{-\gamma_m(\lambda) z} , \tag{4}$$

with $\gamma_m(\lambda)$ given by the empirical formula [11,12]:

$$\gamma_m(\lambda) = \gamma_1(\lambda) + \gamma_1(\lambda) I_\rho \left\{ \eta [m / M(\lambda) - 1 / M(\lambda)]^{2\alpha/(\alpha+2)} \right\}, \tag{5}$$

$\gamma_1(\lambda)$ denotes the attenuation of the first mode, $I_\rho(\cdot)$ is the ρth-order modified Bessel function of the first kind and η is a weighting constant. ρ and η are calculated with measured DMA profiles as described in [9], where a general DMA profile is given. In order to calculate the absolute attenuation for each mode, $\gamma_1(\lambda)$ has to be estimated. This may be done taking into account measurement results of [1], where the total attenuation coefficient $\Gamma(\lambda)$ of a monochromatically excited POF, is given. The total received power at a wavelength λ equals the sum of individual received powers from all excited modes, that is:

$$\sum_{m=1}^{M(\lambda)} e^{-\gamma_m(\lambda) z} = 10^{-\Gamma(\lambda) z} . \tag{6}$$

The received power is found by relation (4) and normalization is applied for (6), considering each mode in the mode group separately and also each wavelength of a response. Finally, calculating $T_m^{-1}(t)$ and $A_m\left[T_m^{-1}(t), z\right]$ for each mode, evaluation of (1) is straightforward.

3. Results and Discussion

For the analytical results, the mathematical simulation program “Mathematica” has been used. For the simulation results, the optical simulation program “VPI Transmission Maker 7.1” has been used, with similar characteristics according to the analytical calculated results for the GI-POF and optical source. Regarding the model for the optical fiber, the optical fiber Module **MultimodeFiber.vtms** from the library of the simulation tool has been used. This model simulates the light propagation through multimode fibers with a refractive index profile either externally specified (a loaded file from real results) or by analytical calculations (Sellmeier function). The optical fiber parameters and characteristics that have been used for both simulation and analytical calculations are a PMMA Ben dopped GI-POF with a core radius w=980 μm, index contrast Δ = 0,01 and core refractive index of 1,45 at a center wavelength of 650 nm in a bandwidth of [620-680] nm is considered. The length of the fiber is considered 0,05 and 0,1 Km and the swap step in the simulation and calculations is 0,1 nm. The refractive indices of the core and the cladding materials follow a three-term Sellmeier function of wavelength with the oscillator strength and oscillator wavelength values are calculated:

$$\mathrm{n_q}(\lambda) = \left(1 + \sum_{k=1}^{3} \frac{A_{q,k}\lambda^2}{\lambda^2 - {\lambda^2}_{q,k}}\right)^{\frac{1}{2}}, \quad q = 1, 2, \tag{7}$$

where $A_{q,k}$ = the oscillator coefficient and $\lambda_{q,k}$ = oscillation wavelength.

A photonic source (RC-LED) of rms spectral width of 2 nm, that is [649, 651] nm emission bandwidth is used and spectral power according to figure 3. The simulation module was the **TxExtMod.vtmg**

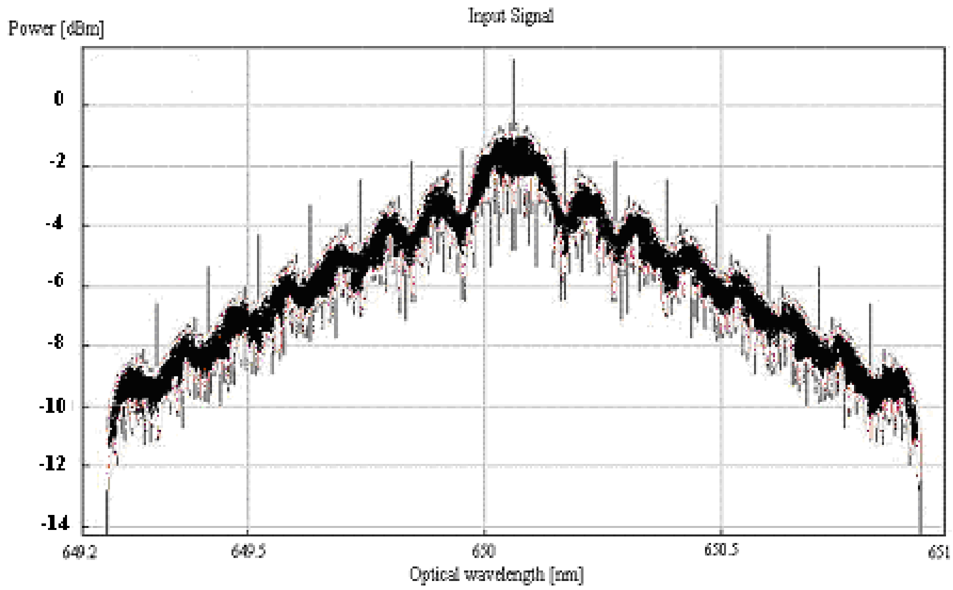

Fig. 3. Optical source (LED) spectral width characteristics

Figure 4 presents the analytically evaluated impulse response of a 50 m and 100 m fiber according to equation (1), based on the described algorithm. It is obvious that the impulse response is narrower in 50 m fiber since the time dispersion is smaller and the supported data rate is increased according to the time-bandwidth product. Moreover time dispersion of a z=100 m GI-POF with the previously described characteristics is calculated analytically almost at 0,2 ns. It is clear that the received power is different for each wave-length according to figure 3, and its curve can be considered to be the impulse response of the channel for an ideal monochromatic optical source of wave-length λ. Following the above calculations and according to the proposed method in this paper, the impulse response of each mode group is calculated with precision. Hence, in figure 4 the overall impulse response is the sum of all such responses of the spectral output of the optical source.

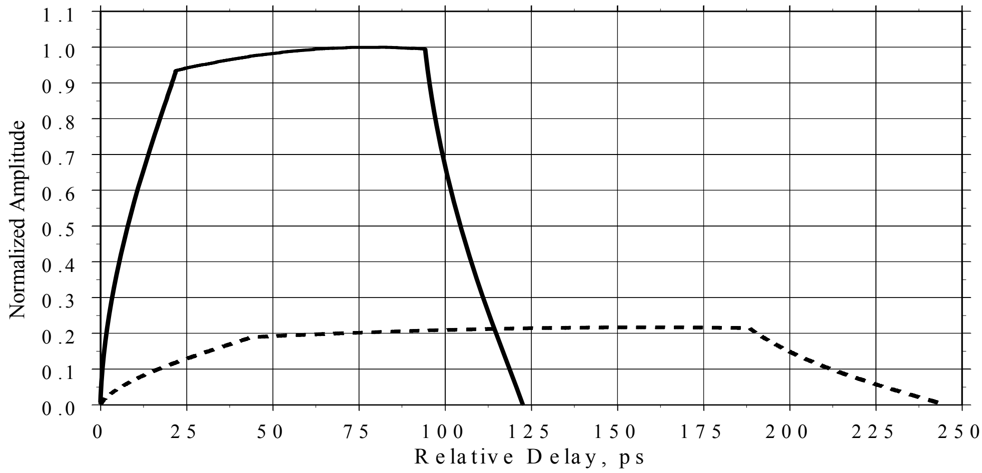

Fig. 4. Analytical Channel impulse response for rms spectral width *5nm, (—) 50m fiber length and (---) 100m respectively*

The results of the Differential Mode Attenuation and the Modal Dispersion are presented in figure 5. The received modal power versus delay time is plotted for three specific wavelengths, l =640, 650 and 660 nm and for the corresponding mode groups according to equation (5). Averaging the different modal powers for each wavelength, for 650 nm received power equals almost -44 dBm, for 640 nm almost -49,5 dBm and for 660 nm almost -51 dBm. It is obvious that the 650 nm wavelength has the maximum modal received power since it is the highest transmitted power according to the optical source spectral width characteristics in figure 3.

Moreover from figure 5 it is also obvious that the modal delay is higher for higher modes of each wavelength. This is expected since, from equation (3), the highest the modes m the highest the modal delay $T_m(\lambda)$.

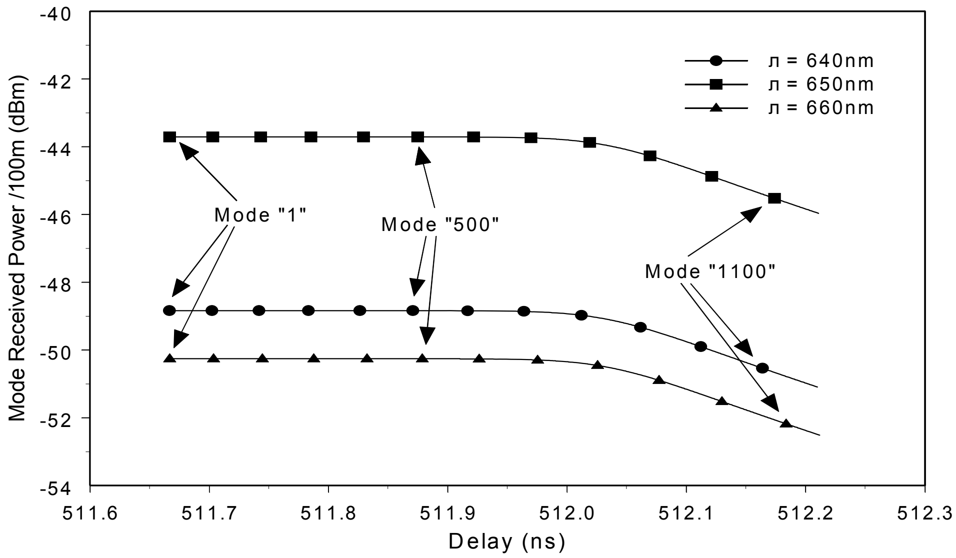

Fig. 5. Analytical calculation of Mode received power versus time delay

Figure 6 presents the output power versus wavelength, where all the different modal groups have been averaged automatically by the simulation tool. The model used by the simulation program is the **Photodiode.vtms,** a model ideal for PIN and APD photodiodes. In this simulation an APD photodiode has been used with thermal sensitivity. The attenuation for 650 nm is almost -44 dBm, for 640 nm almost -54.5 dBm and for 660 nm almost -54 nm. Comparing these results with the analytical, calculated ones from figure 5, it is obvious that the deviation is very small, thus simulation results approve the analytical calculations. Figure 7 shows the electrical characteristics of a 10 Gbps input signal to the RC-LED optical source and figure 8 shows the electrical response of the APD photodiode. It is obvious that the received signal is corrupted mainly due to the multimode - multipath effects (time dispersion characteristics of the channel), the chromatic dispersion effects of the channel (dispersive channel) and the mode coupling effects. Especially the time dispersion results in the time broadening of the time pulses. Indeed, from figures 7 and 8, the time pulse transmitted with a time duration $\Delta T = 3.9 - 3.25 = 0{,}65$ ns is received with a $\Delta T = 3.2 - 2.2 = 1$ ns time duration, resulting into a D = 1ns – 0.65 ns = 0.35 ns broadening. Moreover, the received signal is also attenuated as expected from the power attenuation characteristics of the GI-PMMA POF channel. The original transmitted signal has been transmitted at 1 mW (almost 0 dBm on the main wavelength λ = 650 nm according to figure 3) and the received signal has been attenuated at the value of $200 \cdot 10^{-6}$ mW (almost -38 dBm on the main wavelength $\lambda = 650$ nm from figure 6).

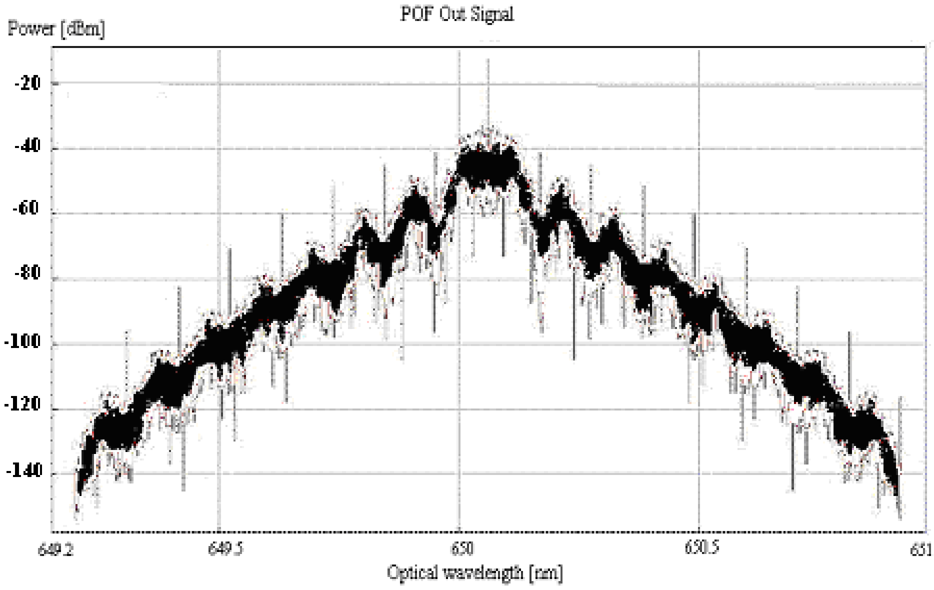

Fig. 6. Received power versus wavelength for a 100m GI-POF length

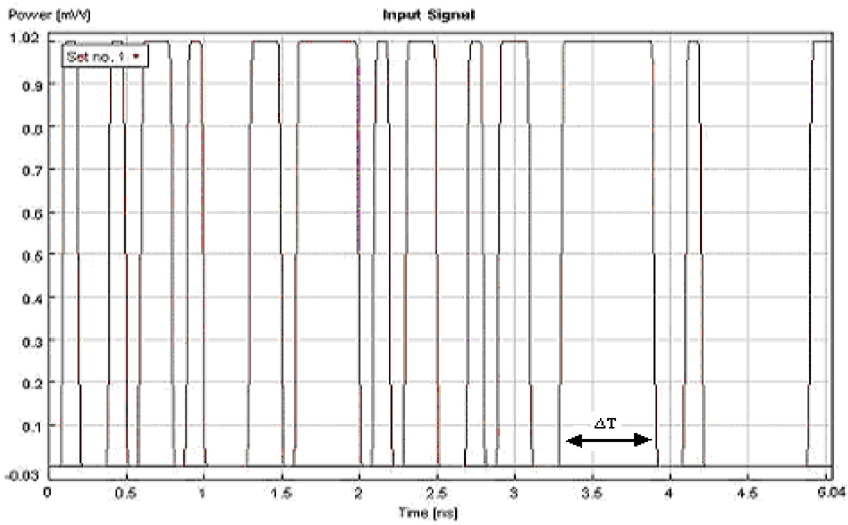

Fig. 7 Input electrical signal for a 100m GI-POF length

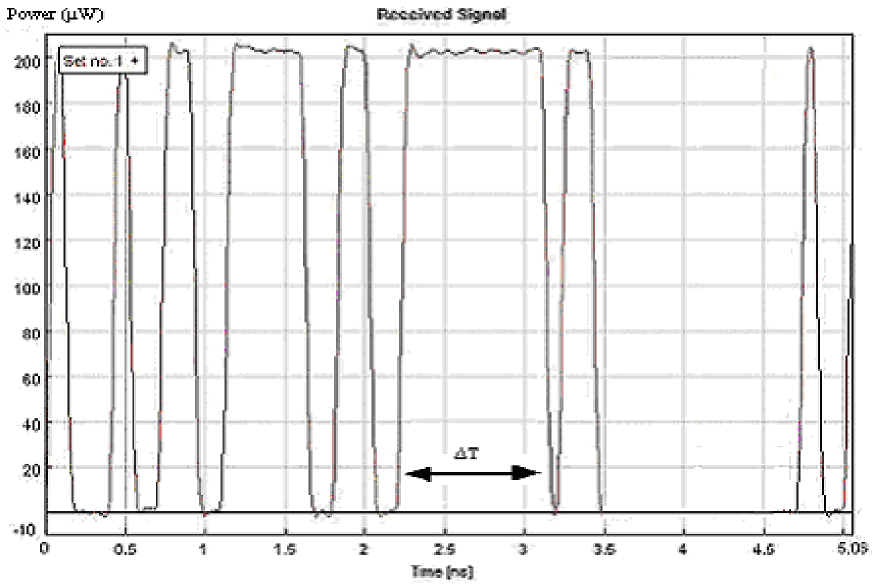

Fig. 8 Received electrical signal for a 100m GI-POF length

4. Conclusions

For indoor coverage the transmission of antenna info through fiber network is important. The use of POF is also advantageous since it is flexible and cost effective. An analytical method has been proposed to calculate the impulse response and the dispersion of the optical channel. The advantage of the proposed method lies in the exact time response provision for any source with known attenuation/wavelength distribution. Thus, it can be used for time domain source pulse shaping investigation, BER calculation and analytical calculation of the characteristics of optical transmission in a GI-POF with proper receiver modeling, and it is a method for end-to-end system modeling and evaluation of GI-POF. Finally, a simulation has been performed to evaluate the characteristics of the channel.

References

[1] W. Andreas, Plastic optical fibers: Principles, Components, Installation, Publicis MCD, Verlag, 2000.

[2] F. Fredricx, Ch. Bouchat, P. Vetter, H.P.A.v.d.Boom, W. Li: Polymer Optical Fiber for data communications: a feasibility study, *Symposium IEEE/LEOS Benelux Chapter*, November 15, 1999, Mons Belgium, ISBN 2-9600226-0-2, pp.115-118.

[3] R. E. Epworth: The Phenomenon of Modal Noise in Analogue and Digital Optical Fiber Communication, *Proc. of 4th European Conf. on Opt. Comm.,* Genoa, Italy, Sept. 1978, pp. 492-501.

[4] T. Ishigure, M. Satoh, O. Takanashi, E. Nihei, T. Nyu, S. Yamazaki, and Y. Koike,: Formation of the Refractive Index Profile in the Graded Index Polymer Optical Fiber for Gigabit Data Transmission, IEEE J. of Lightwave Tech., vol. **15**, no. 11, Nov. 1997, pp. 2095-2100.

[5] Y. Koike, T. Ishigure and E. Nihei,: High-bandwidth graded-index polymer optical ficer, IEEE J. Lightwave Technol., vol 13, no. 7, 1995, pp. 1475-1489

[6] T. Nakamura et al.: VCSELs for Home Networks – Applications of 780 nm VCSEL for POF, POF-2003 proceedings, Seattle September 15-17, 2003, p. 161

[7] W. Li, G. Khoe, H.v.d. Boom, G. Yabre, H. de Waardt, Y. Koike, S. Yamazaki, K. Nakamura, Y. Kawaharada,: 2.5 Gbit/s Transmission over 200 m PMMA Graded Index Polymer Optical Fiber Using a 645 nm Narrow Spectrum Laser and a Silicon APD, Microwave and Optical technology letter, vol. 20, No. 3, Febr. 5 1999, pp 163-166

[8] S. Louvros; A.C. Iossifides; G. Economou; G.K. Karagiannidis; S.A. Kotsopoulos; D. Zevgolis, Time domain modelling and characterizetion of polymer optical fibers, IEEE Photonics Technology Letters, vol. **16**, Issue 2, Feb. 2004, 455-457.

[9] A.R. Mickelson and M. Eriksrud,, Mode-Dependent Attenuation in optical fibers, J. Opt. Soc. Am., vol. **73**, no. 19, Oct. 1983, 1282-1290.

[10] R. Olshansky, and D.B. Keck, Pulse Broadening in Graded-Index Optical Fibers, Applied Optics, vol. **15**, no.2, Feb. 1976, 483-491.

[11] G. Yabre, Comprehensive Theory of Dispersion in Graded-Index Optical Fibers, IEEE J. of Lightwave Tech., vol. **18**, no. 2, Feb. 2000, 166-177.

[12] G. Yabre, Theoretical Investigation on the Dispersion of Graded-Index Polymer Optical fibers, IEEE J. of Lightwave Tech., vol. **18**, no. 6, June 2000, 869-877.

Received: July, 2008